

Niobium-doped titanium oxide anode and ionic liquid electrolyte for a safe sodium-ion battery

Hiroyuki Usui^{†,§}, Yasuhiro Domi^{†,§}, Masahiro Shimizu^{†,§}, Akinobu Imoto^{†,§}, Kazuki Yamaguchi, Hiroki Sakaguchi^{,†,§}*

[†] Department of Chemistry and Biotechnology, Graduate School of Engineering,
Tottori University, 4-101 Minami, Koyama-cho, Tottori 680-8552, Japan

[§] Center for Research on Green Sustainable Chemistry
Tottori University, 4-101 Minami, Koyama-cho, Tottori 680-8552, Japan

Corresponding Author

* Tel./Fax: +81-857-31-5265, E-mail: sakaguch@chem.tottori-u.ac.jp

ABSTRACT

The anode properties of Nb-doped rutile TiO₂ electrodes were investigated in an ionic liquid electrolyte comprised of *N*-methyl-*N*-propylpyrrolidinium cation and bis(fluorosulfonyl)amide anion for use in a safe Na-ion battery. Although the electrolyte's conductivity was lower than that of a conventional organic electrolyte at 30 °C, it showed high conductivity comparable to that of the organic electrolyte at 60 °C. The Nb-doped TiO₂ electrode showed excellent cyclability in the ionic liquid electrolyte at 60 °C: a high capacity retention of 97% was observed even at the 350th cycle, which is comparable to value in the organic electrolyte (91%). In a non-flammability test in a closed system, no ignition was observed with the ionic liquid electrolyte even at 300 °C. These results indicate that combination of a Nb-doped TiO₂ anode and ionic liquid electrolyte gives not only an excellent cyclability but also high safety for a Na-ion battery operating at a temperature below the sodium's melting point of 98 °C.

KEYWORDS. Na-ion battery; Rutile-type titanium oxide; Anode material; Ionic liquid electrolyte; Non-flammability

Introduction

Na-ion batteries (NIBs) are the most promising candidates for the near-term replacement of Li-ion batteries (LIBs) in stationary storage systems because sodium resources are nearly inexhaustible, available at much lower cost than lithium resources, and well-distributed geographically [1,2]. Unlike batteries in portable electronic devices, stationary storage devices require a long-term cycle stability and a high safety rather than a high energy density. For large-scale stationary battery, a sodium–sulfur battery [3] has been shown to offer the advantages of a low cost and a long charge–discharge cycle life. However, this battery requires a high operating temperature above 300 °C to achieve a sufficient ionic conductivity for its solid electrolyte consisting of Na-conductive β -alumina. At such a high temperature, molten sodium and sulfur are highly corrosive. Thus, although a sodium–sulfur battery has great advantages with respect to low cost, high capacity, and environmental friendliness, it still presents a safety issue. Therefore, for the development of a home storage battery, researchers have been interested in NIBs that operate below sodium's melting point of 98 °C, and have investigated various materials for their potential applications in the anode, cathode, and electrolyte [4-9].

The electrolyte strongly affects many of the performance characteristics of batteries. Compared to conventional organic electrolytes comprised of carbonate solvents, ionic liquid electrolytes have many interesting properties such as a wider electrochemical potential window, a better thermal stability, a non-volatility, and consequent non-flammability. If we wish to use ionic liquids as electrolytes in batteries, we should evaluate not only the electrolytes themselves but also cell performance when these electrolytes are used in combination with electrodes consisting of different materials. However, only a few studies have examined the combination of cathode

materials and ionic liquid electrolytes for use in a Na-ion battery [7,10-13]. In contrast, our group has reported that the use of some ionic liquid electrolytes with cations of pyrrolidinium or piperidinium can improve the anode properties not only for LIB electrodes based on Si [14-18], but also for NIB electrodes consisting of P [19] and Sn-P [20]. One possible explanation for this result is that a uniform surface layer is formed on the electrodes because of their high electrochemical stability, and lithiation and sodiation occur over entire surface of the electrodes to suppress electrode disintegration [8].

We have recently found that rutile-type TiO_2 is a potential anode material for use in NIBs [21]. Due to its low cost, high abundance, and ready availability, it is expected that TiO_2 could be useful as an anode material in NIBs. We previously revealed that niobium (Nb)-doping in rutile TiO_2 increased its electronic conductivity 1000-fold and improved NIB anode performance [21]. However, we investigated this performance only in a conventional organic solvent. With respect to battery safety, its performance in an ionic liquid electrolyte would be very interesting. In this study, we studied the anode performance of a rutile TiO_2 electrode in a pyrrolidinium-based ionic liquid electrolyte. We also focused on a method for evaluating the electrolyte's flammability, since this has never been standardized even though the evaluation conditions are extremely important. We strongly believe that the flammability test should be standardized as soon as possible for the early application of NIBs. Thus, we evaluated the electrolyte's flammability by a new method which has been standardized and is much more accurate than conventional methods.

Experimental

As an active material powder, Nb-doped rutile TiO₂ (Ti_{0.94}Nb_{0.06}O₂) particles were synthesized by a typical sol–gel method. For the evaluation of NIB anode properties, Nb-doped TiO₂ thick-film electrodes were prepared by a gas-deposition (GD) method that did not include any binder or conductive material [22,23]. The conditions for active material synthesis and electrode preparation were described in our previous paper [21].

2032-type coin cells were assembled using a Nb-doped TiO₂ electrode as the working electrode, a Na foil counter electrode, an electrolyte, and a glass fiber separator. As an ionic liquid electrolyte, we used 1 M sodium bis(fluorosulfonyl)amide (NaFSA, Mitsubishi Materials Electronic Chemicals Co., Ltd.) dissolved in *N*-methyl-*N*-propylpyrrolidinium-bis(fluorosulfonyl)amide (Py13-FSA, Kishida Chemical Co., Ltd.). For comparison, we studied 1 M NaFSA dissolved in propylene carbonate (PC; C₄H₆O₃, Kishida Chemical Co., Ltd.) as a conventional organic electrolyte. Galvanostatic charge–discharge tests were performed under a current density of 50 mA g⁻¹ (0.15C) in a potential range between 0.005 and 3.000 V vs. Na⁺/Na at 30 °C and 60 °C.

The electric conductivity of the electrolytes was measured at a temperature range from 20 °C to 80 °C by an electrochemical impedance instrument (CompactStat, Ivium Technologies) through a two-electrode-type cell equipped with two platinum electrodes. To demonstrate the non-flammability of the ionic liquid electrolyte, we conducted a fire-resistance test by using a closed-cup flash point tester (Setaflash Series: 33000-0, Stanhope-Seta Ltd.). In a previous study, we confirmed the non-flammability of an ionic liquid electrolyte by using this test for the first time [19]. The results of this test are very reproducible and the test itself has been standardized according to Japanese Industrial Standards (JIS) K2265-2, which corresponds to International Organization for Standardization (ISO) 3679:2004 i.e., the “Rapid equilibrium closed cup method”. The test procedures were explained in the previous paper [19].

Results and Discussion

Figure 1 shows the results of electric conductivity measurements for electrolytes consisting of NaFSA/Py13-FSA and NaFSA/PC. At 30 °C, the NaFSA/Py13-FSA electrolyte showed a conductivity of 4.95 mS cm⁻¹, which is lower than that for the NaFSA/PC electrolyte (8.55 mS cm⁻¹). At 60 °C, NaFSA/Py13-FSA showed an increase in conductivity to 11.9 mS cm⁻¹, which is close to the value obtained for NaFSA/PC (13.6 mS cm⁻¹). In general, ionic liquid electrolytes show much lower conductivity than organic electrolytes due to their stronger electrostatic interaction between cations and anions. In this study, we confirmed that NaFSA/Py13-FSA electrolyte exhibited conductivity comparable to that of an organic electrolyte when the temperature was increased to around 60 °C. Temperatures close to 60 °C are beneficial for practical

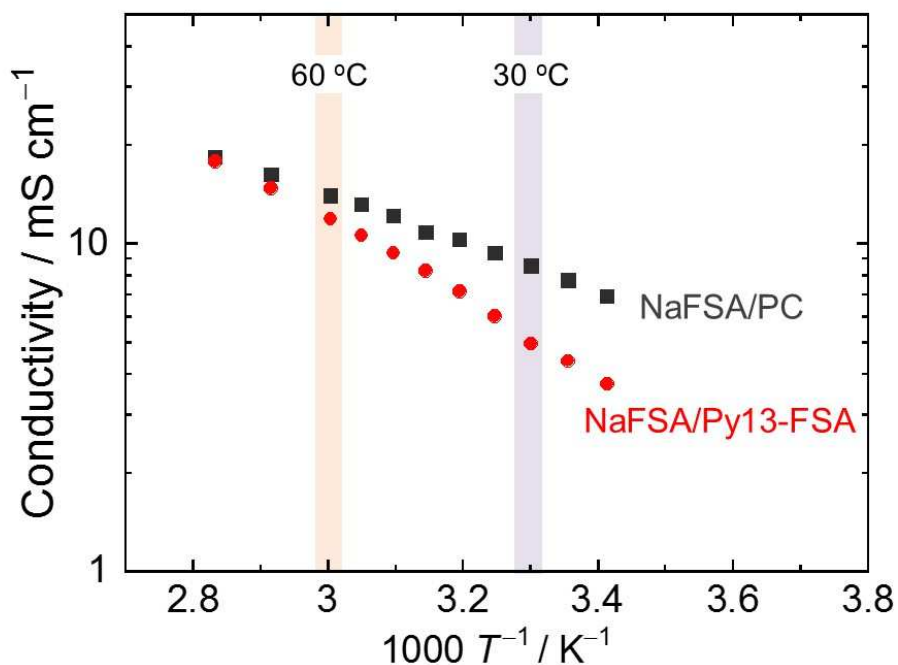


Figure 1. Temperature-dependence of electric conductivity for electrolytes consisting of NaFSA/Py13-FSA and NaFSA/PC at a concentration of 1.0 M.

application because they can be easily achieved by exhaust heat from homes, office buildings, and factories without any additional heating apparatus.

Figure 2 presents the charge–discharge profiles of Nb-doped TiO₂ electrodes at 30 °C and 60 °C in the different electrolytes. In the initial charge (sodiation) profiles at 30 °C, long potential slopes appeared below 1.0 V vs. Na⁺/Na for the electrolytes of NaFSA/Py13-FSA and NaFSA/PC, resulting in large irreversible capacities in the first cycle. This would reflect cathodic electrolyte decomposition and the formation of a solid–electrolyte interface layer [24]. After the second cycle, gentle potential slopes were repeatedly observed at 0–0.7 V and 0.7–1.5 V in the charge and discharge (delithiation) profiles, respectively. These slopes originate from the Na-insertion and Na-extraction of rutile TiO₂ [21]. With a rise in temperature from 30 °C to 60 °C, the initial reversible capacities of 110 and 120 mA h g⁻¹ for Py13-FSA and PC increased to 180 and 200 mA

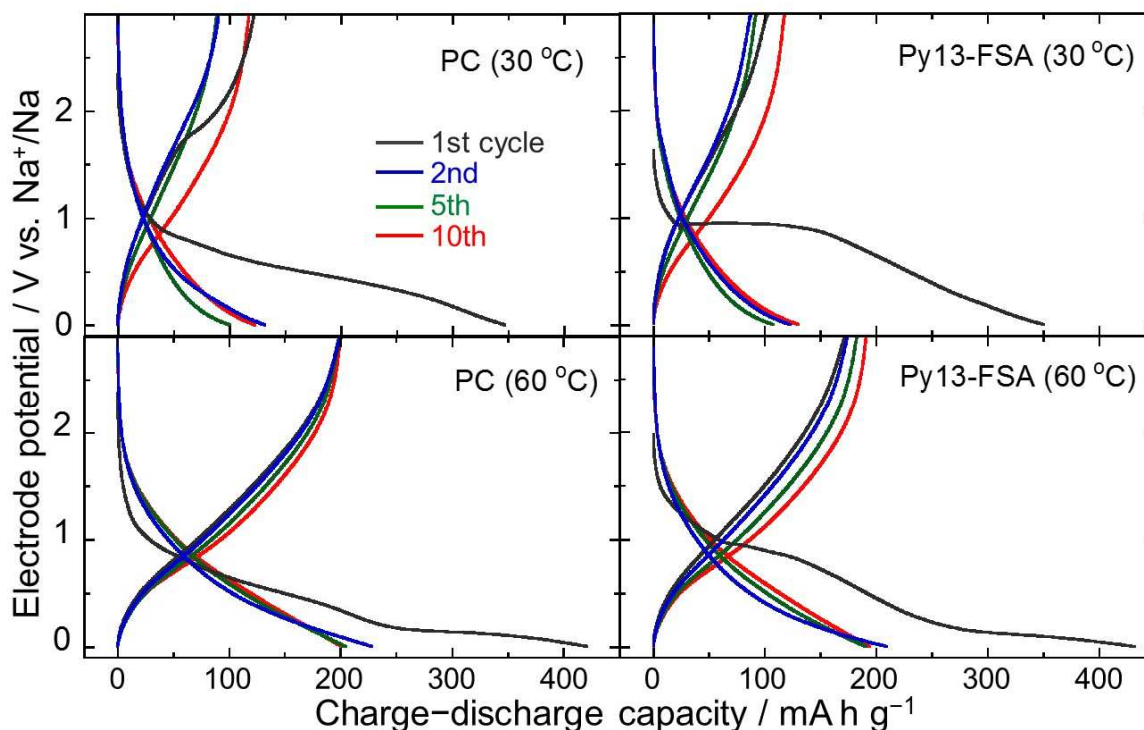


Figure 2. Charge–discharge curves of Nb-doped TiO₂ electrodes in the electrolytes under 50 mA g⁻¹ (0.15C) at 30 °C and 60 °C.

h g^{-1} , respectively. Their high-rate performances (Fig. S1) indicates that Na-ion diffusion in the electrolyte is one of the rate-determining steps in the electrode reaction. The enhanced conductivity of the electrolyte at the higher temperature probably increased the charge–discharge capacities.

Figure 3 represents cycling performance of the electrodes. In the cycling tests at 30 °C, the discharge capacities gradually increased during the initial 20 cycles in each electrolyte. Coulombic efficiencies progressively increased and reached 100% at the 20th cycle (Fig. S2), suggesting that the electrolyte decomposition reaction disturbed the sodiation/desodiation of Nb-doped TiO_2 until the 20th cycle. In NaFSA/Py13-FSA at 60 °C, the electrode exhibited a remarkably improved performance with a capacity retention of 97% even after 350 cycles. This cycling performance is nearly equivalent to that observed for NaFSA/PC at 60 °C, for which the capacity retention was

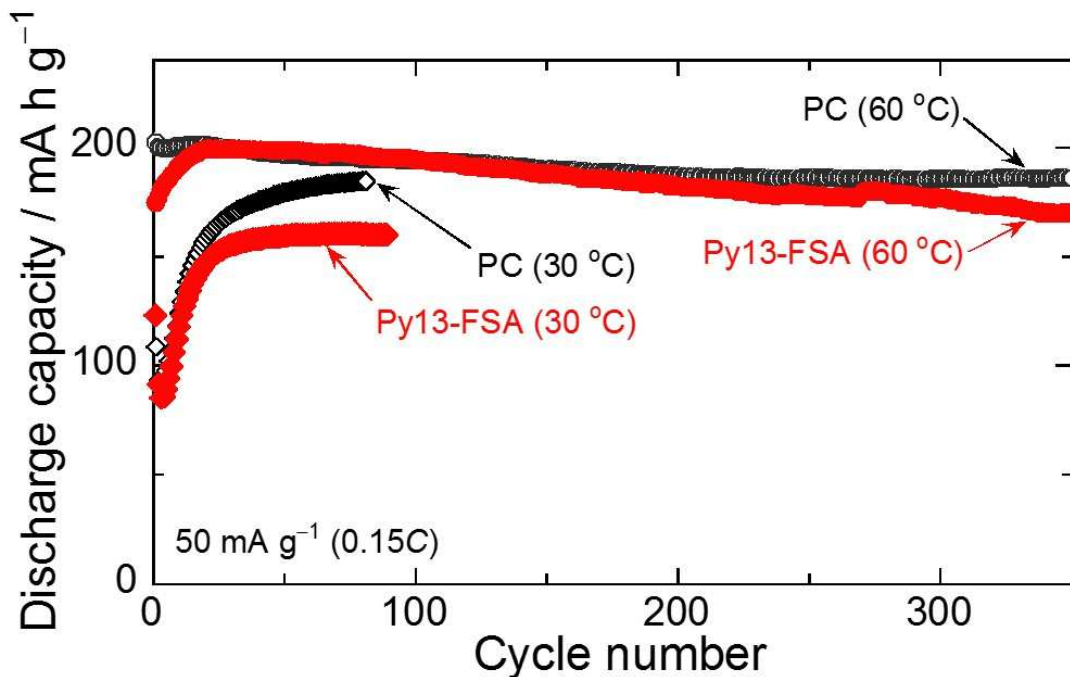


Figure 3. Cycling performances of Nb-doped TiO_2 electrodes in electrolytes consisting of NaFSA/PC and NaFSA/Py13-FSA at temperatures of 30 °C and 60 °C.

91% at the 350th cycle. Note that the much safer electrolyte based on an ionic liquid showed performance comparable to that of a conventional organic electrolyte below sodium's melting point of 98 °C.

The most attractive advantage of an ionic liquid electrolyte is its non-flammability, which arises from the strong electrostatic interaction between the cation and anion and the resulting non-volatility. Many researchers have extensively evaluated non-flammability by direct contact with a pilot flame [25-31]. This test is simple and observable. However, these flammability tests were performed under unstandardized conditions: the test conditions can differ dramatically such as with respect to amount of ionic liquid, the flame temperature, the distance between the ionic liquid and the flame, the duration of flame contact. Thus, it is impossible to compare these results. In addition, as a critical point, all of these flammability tests were performed in an open system [25-31]. The gas concentration of a thermally decomposed ionic liquid does not easily reach its combustion limit in an open system, which leads to an underestimation of its non-flammability. Thus, we newly introduced a closed-system flammability test [19] and an international standardized condition. Figure 4 displayed the results of the closed-cup flash point test for the electrolytes used here. The NaFSA/PC organic electrolyte showed an explosive combustion at 150 °C, which is close to the flash point of PC (132 °C). No ignition was observed for the NaFSA/Py13-FSA ionic liquid electrolyte even at 300 °C (see video in Supporting Information), which clearly demonstrates its non-flammability. Our test can be performed in a closed system similar to the

conditions for practical battery. Based on the JIS and ISO standards, the test gives a correct flash point and reliable reproducibility.

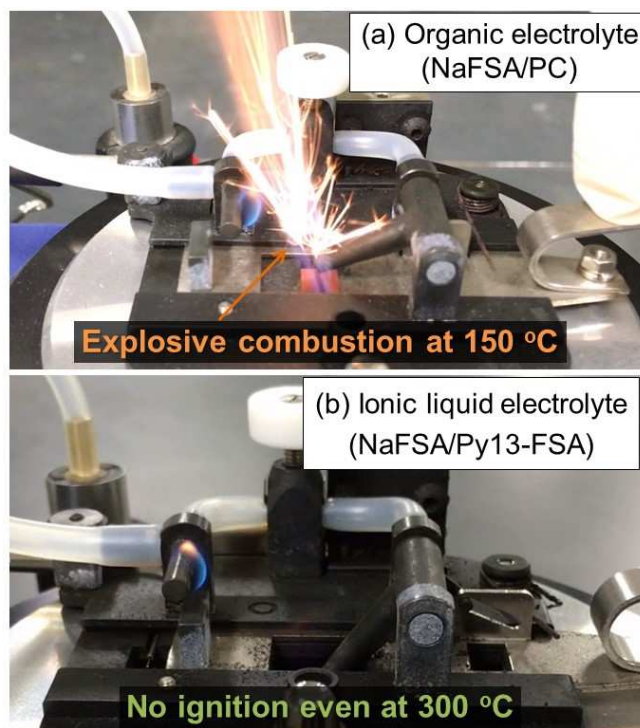


Figure 4. Results of closed-cup flash point test for the electrolytes. The tests were performed based on the standards of JIS K2265-2 and ISO 3679:2004.

Conclusions

The electrochemical properties of a Nb-doped TiO₂ electrode and NaFSA/Py13-FSA ionic liquid were investigated for use as an anode and electrolyte in a highly safe Na-ion battery. Conductivity measurements at 30 °C revealed that the value for NaFSA/Py13-FSA (4.95 mS cm⁻¹) was lower than that for NaFSA/PC (8.55 mS cm⁻¹). With an increase in temperature to 60 °C, the conductivity of ionic liquid electrolyte increased to 11.9 mS cm⁻¹, which is close to the value observed for

NaFSA/PC (13.6 mS cm⁻¹). The potential performance of a Nb-doped TiO₂ anode was successfully exerted with an increase in temperature from 30 °C to 60 °C. A significantly improved cyclability and high capacity retention of 97% at the 350th cycle were achieved with the ionic liquid electrolyte at 60 °C, which are comparable to the performance and retention (91%) observed for the organic electrolyte. We revealed for the first time that electrode performance can be improved at an elevated temperature for a combination of a Nb-doped TiO₂ anode and an ionic liquid electrolyte. In addition, we introduced a closed-system flammability test and international standardized conditions, in contrast to the conventional open-system tests. These results should contribute to the development of a safe Na-ion battery based on an ionic liquid electrolyte.

ACKNOWLEDGMENT

This work was partially supported by the Japan Society for the Promotion of Science (JSPS) KAKENHI Grant numbers 24350094, 15K21166, and 16K05954. This work was supported by the "Joint Usage/Research Program on Zero-Emission Energy Research, Institute of Advanced Energy, Kyoto University ZE27A-21 and ZE28A-21", the Japan Association for Chemical Innovation (JACI), and the Izumi Science and Technology Foundation.

References

- [1] S. Komaba, W. Murata, T. Ishikawa, N. Yabuuchi, T. Ozeki, T. Nakayama, A. Ogata, K. Gotoh, K. Fujiwara, *Adv. Funct. Mater.*, **21** (2011) 3859–3867.
- [2] B. L. Ellis, L. F. Nazar, *Curr. Opin. Solid State Mat. Sci.*, **16** (2012) 168–177.
- [3] T. Oshima, M. Kajita, A. Okuno, *Int. J. Appl. Ceram. Technol.*, **1** (2004) 269–276.

- [4] T. Yamamoto, T. Nohira, R. Hagiwara, A. Fukunaga, S. Sakai, K. Nitta, S. Inazawa, *J. Power Sources*, **237** (2013) 98–103.
- [5] D. Monti, E. Jónsson, M. R. Palacín, P. Johansson, *J. Power Sources*, **245** (2014) 630–636.
- [6] C.-Y. Chen, K. Matsumoto, T. Nohira, R. Hagiwara, Y. Orikasa, Y. Uchimoto, *J. Power Sources*, **246** (2014) 783–787.
- [7] C. Ding, T. Nohira, R. Hagiwara, K. Matsumoto, Y. Okamoto, A. Fukunaga, S. Sakai, K. Nitta, S. Inazawa, *J. Power Sources*, **269** (2014) 124–128.
- [8] A. Ponrouch, M. R. Palacín, *Electrochem. Commun.*, **54** (2014) 51–54.
- [9] I. Hasa, S. Passerini, J. Hassoun, *J. Power Sources*, **303** (2016) 203–207.
- [10] L. G. Chagas, D. Buchholz, L. Wu, B. Vortmann, S. Passerini, *J. Power Sources*, **247** (2014) 377–383.
- [11] N. Wongittharom, C. Wang, Y. Wang, C. Yang, J. Chang, *ACS Appl. Mater. Interfaces*, **6** (2014) 17564–17570.
- [12] N. Wongittharom, T. Lee, C. Wang, Y. Wang, J. Chang. *J. Mater. Chem. A*, **2** (2014) 5655–5661.
- [13] C. Wang, Y. Yeh, N. Wongittharom, Y. Wang, C. Tseng, S.-W. Lee, W.-S. Chang, J.-K. Chang, *J. Power Sources*, **274** (2015) 1016–1023.
- [14] H. Usui, Y. Yamamoto, K. Yoshiyama, T. Itoh, H. Sakaguchi, *J. Power Sources*, **196** (2011) 3911–3915.
- [15] H. Usui, T. Masuda, H. Sakaguchi, *Chem. Lett.*, **41** (2012) 521–522.
- [16] H. Usui, M. Shimizu, H. Sakaguchi, *J. Power Sources*, **235** (2013) 29–35.
- [17] M. Shimizu, H. Usui, K. Matsumoto, T. Nokami, T. Itoh, H. Sakaguchi, *J. Electrochem. Soc.*, **161** (2014) A1765–A1771.

- [18] M. Shimizu, H. Usui, T. Suzumura, H. Sakaguchi, *J. Phys. Chem. C*, **119** (2015) 2975–2982.
- [19] M. Shimizu, H. Usui, K. Yamane, T. Sakata, T. Nokami, T. Itoh, H. Sakaguchi, *Int. J. Electrochem. Sci.*, **10** (2015) 10132–10144.
- [20] H. Usui, T. Sakata, M. Shimizu, H. Sakaguchi, *Electrochemistry*, **83** (2015) 810–812.
- [21] H. Usui, S. Yoshioka, K. Wasada, M. Shimizu, H. Sakaguchi, *ACS Appl. Mater. Interfaces*, **7** (2015) 6567–6573.
- [22] H. Sakaguchi, T. Toda, Y. Nagao, T. Esaka, *Electrochem. Solid-State Lett.*, **10** (2007) J146–J149.
- [23] H. Usui, Y. Kiri, H. Sakaguchi, *Thin Solid Films*, **520** (2012) 7006–7010.
- [24] K.-T. Kim, G. Ali, K. Y. Chung, C. S. Yoon, H. Yashiro, Y.-K. Sun, J. Lu, K. Amine, S.-T. Myung, *Nano Lett.*, **14** (2014) 416–422.
- [25] B. S. Lalia, N. Yoshimoto, M. Egashira, M. Morita, *J. Power Sources*, **195** (2010) 7426–7431.
- [26] C. Arbizzani, G. Gabrielli, M. Mastragostino, *J. Power Sources*, **196** (2011) 4801–4805.
- [27] G. Nagasubramanian, K. Fenton, *Electrochim. Acta*, **101** (2013) 3–10.
- [28] H. Li, J. Pang, Y. Yin, W. Zhuang, H. Wang, C. Zhai, S. Lu, *RSC Adv.*, **3** (2013) 13907–13914.
- [29] I. Quinzeni, S. Ferrari, E. Quartarone, C. Tomasi, M. Fagnoni, P. Mustarelli, *J. Power Sources*, **237** (2013) 204–209.
- [30] M. Montanino, M. Moreno, M. Carewska, G. Maresca, E. Simonetti, R. Lo Presti, F. Alessandrini, G. B. Appetecchi, *J. Power Sources*, **269** (2014) 608–615.
- [31] B. Yang, C. Li, J. Zhou, J. Liu, Q. Zhang, *Electrochim. Acta*, **148** (2014) 39–45.